



# 21st Century alpine climate change

Sven Kotlarski<sup>1</sup> · Andreas Gobiet<sup>2</sup> · Samuel Morin<sup>3</sup> · Marc Olefs<sup>2</sup> · Jan Rajczak<sup>1,4</sup> · Raphaëlle Samacoïts<sup>5</sup>

Received: 30 September 2021 / Accepted: 17 April 2022

© The Author(s) 2022

## Abstract

A comprehensive assessment of twenty-first century climate change in the European Alps is presented. The analysis is based on the EURO-CORDEX regional climate model ensemble available at two grid spacings (12.5 and 50 km) and for three different greenhouse gas emission scenarios (RCPs 2.6, 4.5 and 8.5). The core simulation ensemble has been subject to a dedicated evaluation exercise carried out in the frame of the CH2018 Climate Scenarios for Switzerland. Results reveal that the entire Alpine region will face a warmer climate in the course of the twenty-first century for all emission scenarios considered. Strongest warming is projected for the summer season, for regions south of the main Alpine ridge and for the high-end RCP 8.5 scenario. Depending on the season, medium to high elevations might experience an amplified warming. Model uncertainty can be considerable, but the major warming patterns are consistent across the ensemble. For precipitation, a seasonal shift of precipitation amounts from summer to winter over most parts of the domain is projected. However, model uncertainty is high and individual simulations can show change signals of opposite sign. Daily precipitation intensity is projected to increase in all seasons and all sub-domains, while the wet-day frequency will decrease in the summer season. The projected temperature change in summer is negatively correlated with the precipitation change, i.e. simulations and/or regions with a strong seasonal mean warming typically show a stronger precipitation decrease. By contrast, a positive correlation between temperature change and precipitation change is found for winter. Among other indicators, snow cover will be strongly affected by the projected climatic changes and will be subject to a widespread decrease except for very high elevation settings. In general and for all indicators, the magnitude of the change signals increases with the assumed greenhouse gas forcing, i.e., is smallest for RCP 2.6 and largest for RCP 8.5 with RCP 4.5 being located in between. These results largely agree with previous works based on older generations of RCM ensembles but, due to the comparatively large ensemble size and the high spatial resolution, allow for a more decent assessment of inherent projection uncertainties and of spatial details of future Alpine climate change.

**Keywords** European Alps · EURO-CORDEX · Climate change · Temperature · Precipitation · Snow cover · Uncertainty

## 1 Introduction

The European Alps stretch about 1200 km across the center of Europe. They are characterized by mountain peaks up to more than 4800 m elevation and deeply incised valleys, and act as a natural barrier to weather systems. They feature important regional climate characteristics (e.g., Schär et al. 1998) induced by orography and land surface characteristics such as the presence of snow and ice and of large inland water bodies. At the same time, the Alps are densely populated and several important economic sectors in the region are highly sensitive to weather and climate. These include tourism, hydropower generation, agriculture, forestry, and water supply. Last but not least, many regions in the Alps are exposed to natural hazards due to gravitational mass

Sven Kotlarski  
sven.kotlarski@meteoswiss.ch

<sup>1</sup> Federal Office of Meteorology and Climatology MeteoSwiss, Zurich-Airport, Switzerland

<sup>2</sup> Zentralanstalt Für Meteorologie Und Geodynamik (ZAMG), Vienna, Austria

<sup>3</sup> Univ. Grenoble Alpes, Université de Toulouse, Météo-France, CNRS, CNRM, Centre d'Études de La Neige, Grenoble, France

<sup>4</sup> Institute for Atmospheric and Climate Science, ETH Zurich, Zurich, Switzerland

<sup>5</sup> Météo-France, Toulouse, France

movements (debris flow, avalanches), which are affected by weather and climate as well. Therefore, weather and climate play a crucial role for millions of people, not only in the Alps themselves, but also in vast surrounding lowland areas (e.g., EEA 2009). Observed warming in the Alps is about twice the global mean (+1.8 °C since 1880; Auer et al. 2007; Begert and Frei 2018). Particularly rapid warming has been observed since the 1980s and seasonal snow (Klein et al. 2016; Marty et al. 2017; Matiu et al. 2021; Olef et al. 2020; Schöner et al. 2018) and glaciers (Beniston et al. 2018; Huss 2012) are retreating. Summer droughts have been shown to intensify (Scherrer et al. 2022). The effects of these changes on society and ecosystems are already observed and the assessment of expected future changes becomes increasingly critical (Hock et al. 2019; Adler et al. 2022). A reliable future projection of these changes is challenging, since mountains feature high spatial variability of climate and surface features and steep vertical gradients. Furthermore, the interaction between the surface and the atmosphere is strong on many spatial scales. The resulting patterns of climate change are often highly complex, small-scale, and demanding in terms of monitoring, modeling, and analysis. Recently, regional climate models (RCMs) have started to resolve scales that roughly account for many of these patterns, although spatial resolution is still too coarse to describe local climate effects in, for example, smaller valleys. Therefore, each new generation of climate simulations with higher spatial resolution than the generation before carries new information and potentially new insights into the mechanisms of climate change in the Alpine region.

This study presents a comprehensive analysis of the projected twenty-first century Alpine climate based on the latest generation of RCMs employed within the EURO-CORDEX initiative (Coppola et al. 2021; Jacob et al. 2014, 2020; Vautard et al. 2021). It can be regarded as an update of the review paper by Gobiet et al. (2014). It furthermore extends the study by Smiatek et al. (2016) by employing a larger model ensemble, by covering a larger set of greenhouse gas scenarios and by additionally discussing elevation-dependence, changes in the character of precipitation, and snow cover. It also extends upon the broader Alpine-scale analysis of Gobiet and Kotlarski (2020) by adding more spatial detail and additional parameters. Our aim is to give a comprehensive overview on expected changes in the climate system of the Alps until the end of the twenty-first century, focusing on annual and seasonal mean changes of near-surface air temperature (simply referred to as temperature in the following), precipitation and snow water equivalent (SWE) as well as on changes of specific precipitation indicators at daily scale. We thereby focus on a rather descriptive presentation of identified changes and their uncertainties and leave a detailed analysis of the governing processes that explain changes in individual indicators to subsequent works. The

analysis is complemented by two exemplary case studies investigating future changes in winter snow depth in the Mont-Blanc region and in the Ötztal Alps, putting one of the most relevant features of Alpine climate change under the microscope. Since the used RCMs have already been evaluated in detail (Kotlarski et al. 2014; Rajczak and Schär 2017; Smiatek et al. 2016), evaluation is not part of this study. We furthermore rely on direct RCM output. With the exception of the two snow cover case studies, the application of impact models (e.g. hydrological models) ingesting RCM results is not part of this work which, however, features indicators that are relevant for estimating the impacts of climate change.

The article is structured as follows: Sect. 2 describes the climate model data that has been analyzed for this study and gives information regarding analysis methods and the study area. Sections 3–6 present the major features of projected climate change in the Alps, ranging from temperature, over precipitation and their extremes, to changes in snow cover. The results are discussed and set into context in Sect. 7, while we end with a brief summary of the main findings and concluding remarks in Sect. 8. Additional information is provided in the accompanying Supplementary Material (Prefix “S” in figure and table numbering).

## 2 Data and methods

### 2.1 Climate model data

Our work is based on a comprehensive set of regional climate simulations that have been performed in the frame of EURO-CORDEX (Jacob et al. 2020), the European branch of the Coordinated Regional Climate Downscaling Experiment (CORDEX; Giorgi et al. 2009; Gutowski et al. 2016). CORDEX is a global initiative that is run under the umbrella of the World Climate Research Programme (WCRP) and that seeks to advance and coordinate the science and application of regional climate downscaling (<https://www.cordex.org>). In particular, CORDEX aims at evaluating and improving regional climate downscaling approaches—explicitly including empirical-statistical methods—and at producing coordinated sets of downscaled projections at regional scale worldwide for use in climate impact assessments. As its European branch, EURO-CORDEX is concerned with climate downscaling over the European continent. In terms of dynamical downscaling, i.e. the application of regional climate models, both reanalysis-driven evaluation simulations and climate change scenarios driven by global climate models (GCMs) under a common simulations protocol and for a pan-European domain are performed (see also <https://www.euro-cordex.net>). The EURO-CORDEX simulation database is publicly available via the nodes of the Earth System Grid

Federation (ESGF; see <https://esgf.llnl.gov>) and via the Copernicus Climate Data Store (<https://cds.climate.copernicus.eu>). It is constantly filled by new simulations and currently includes more than 100 regional climate simulations at spatial resolutions of 12.5 km ( $0.11^\circ$  on a rotated grid; EUR-11 sub-ensemble) and 50 km ( $0.44^\circ$  on a rotated grid; EUR-44 sub-ensemble) spanning a historical period plus the entire twenty-first century. The boundary forcing is provided by GCM simulations of the Coupled Model Intercomparison Project 5 (CMIP5; Taylor et al. 2012), driven by historical greenhouse gas concentrations until the year 2005 and assuming three distinct greenhouse gas scenarios (in the following also referred to as emission scenarios) for the period 2006–2100: representative concentration pathways RCPs 2.6, 4.5 and 8.5 (Moss et al. 2010). These scenarios range from a mitigation scenario implying rapid and substantial reductions in global greenhouse gas emissions (RCP 2.6) to large and unabated emissions until the end of the twenty-first century (RCP 8.5). Among others, the EURO-CORDEX simulation ensemble has been employed in national climate change assessments in the Alpine region (CH2018 2018; Chimani et al. 2020). In the future CORDEX will continue to downscale GCM simulations as a dedicated model intercomparison project endorsed by the Coupled Model Intercomparison Project 6 (CMIP6; Gutowski et al. 2016).

We here deliberately refrain from evaluating the performance of the EURO-CORDEX models in the historical period over the Alpine region but, instead, refer to previous works that carried out such evaluations and that found on overall good agreement with observational references but also important and partly systematic model biases (e.g., CH2018 2018; Kotlarski et al. 2014; Smiatek et al. 2016; Vautard et al. 2021). Furthermore, individual simulations were shown to be subject to unphysical behavior. As a consequence, we do not by default exploit the full EURO-CORDEX simulation ensemble that is presently available but rely on the EURO-CORDEX model sub-ensemble that has been evaluated, tested and finally employed in the CH2018 Climate Scenarios for Switzerland (CH2018 2018; Sørland et al. 2020; Fischer et al. 2022). This set corresponds to all model runs available at the end of the year 2017 except for simulations excluded due to quality issues. The CH2018 model set also includes a spatial filtering of model output of the SMHI-RCA4 and DMI-HIRHAM5 RCMs in order to reduce spatial noise in precipitation change patterns. Simulations that are not provided on the standard EURO-CORDEX rotated grids (EUR-11 and EUR-44) were conservatively remapped to these standard grids. See the CH2018 Technical Report for further details on the ensemble choice and the spatial filtering and remapping (CH2018 2018; Sect. 4.2.1 therein). The final model ensemble used in CH2018 and in the present work consists of 68 simulations performed by 7 different RCMs that are, in turn, driven by 12 different

GCMs (Table S1 in the Supplementary Material). 24 of these simulations were carried out at the higher 12.5 km resolution, 44 simulations at the coarser 50 km grid spacing. For all simulations the common output period 1971–2099 and the variables near-surface air temperature (tas; monthly mean values), total precipitation (pr; daily and monthly sums) and snow water equivalent (snw; monthly mean values) were analyzed.

For the Alpine snow cover analysis the available model ensemble was further reduced. First, due to the pronounced height dependency of snow cover and its control by temperature thresholds, only the high-resolution EUR-11 simulations were considered. Second, additional quality criteria were applied, leading to a removal of simulations with persistent snow accumulation at high elevation grid cells. Again we refer to the CH2018 Technical Report for further details (CH2018 2018; Sect. 4.6 therein). The final sub-ensemble considered in the Alpine snow analysis consists of 12 simulations (Table S1 in the Supplementary Material). In order to fully exploit a maximum number of simulations available and to optimally assess model uncertainty, a larger ensemble—partly using EURO-CORDEX simulations produced after the time of production of CH2018—has been used for the Mont-Blanc and Ötztal Alps snow case studies (Sects. 6.2 and 6.3; see Table S1). Note that for all ensembles the number of simulations used in the analysis of each of the three emission scenarios differs. Hence, the intercomparison of results for the individual emission scenarios is not fully consistent.

## 2.2 Analysis domain

The EURO-CORDEX simulations are available on a pan-European model domain stretching from the North Atlantic in the West to the Black Sea in the East and from the northern tip of Scandinavia to Northern Africa (see e.g. Kotlarski et al. 2014). For the present work a rectangular sub-domain covering the entire Alpine region has been extracted from the model grids of both the high-resolved EUR-11 ensemble and the coarse-resolved EUR-44 ensemble (Fig. 1). While the resolution of the former is able to represent the main orographic features of the Alps and extends to elevations above 3000 m a.s.l. (Fig. 1, upper panel), the EUR-44 resolution represents the Alpine orography only very roughly and in particular does not cover elevations above about 2500 m a.s.l. (Fig. 1, middle panel). Sea grid cells are excluded from any analysis.

For the spatially averaged derivation of climate change signals, three distinct sub-regions covering the Alpine ridge plus adjacent lowlands are used (see Fig. 1, lower panel): the Northeastern Alps (Alps NE), the Northwestern Alps (Alps NW) and the Southern Alps (Alps S) as defined in a previous work by Rajczak et al. (2013). These

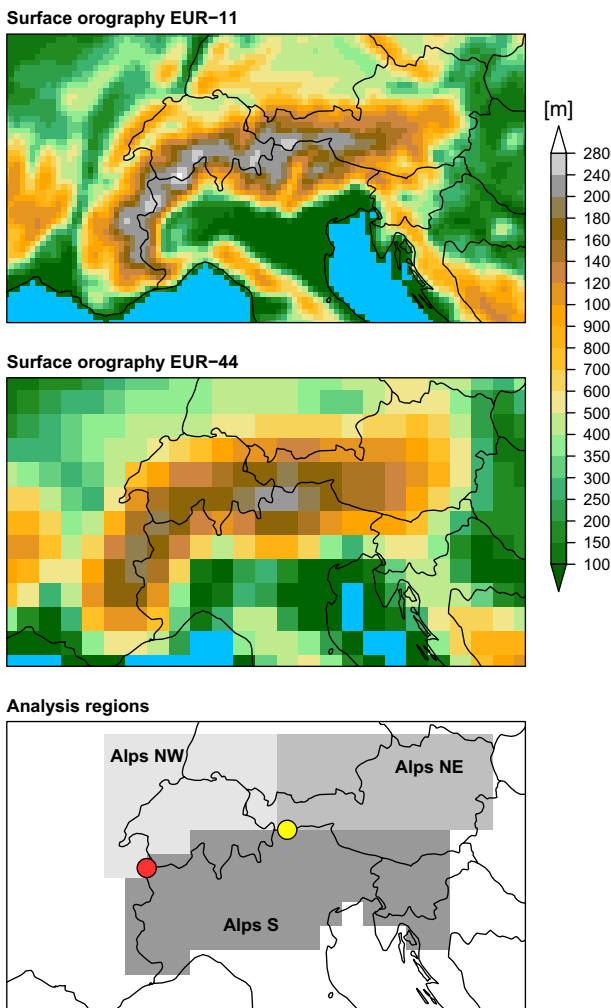


**Fig. 1** Upper and middle panel: orography of the Alpine region [m] as extracted from the standard EUR-11 (top) and EUR-44 (middle) EURO-CORDEX model domains. For illustrative purposes the surface orography of one particular RCM is shown (CLMcom-CLM4-8-17). Oroographies of other RCMs can slightly differ. Lower panel: individual sub-regions used for spatially averaged analyses. The colored circles show the locations of the Mont-Blanc massif (red) and the Ötztal Alps (yellow) for which dedicated snow cover analyses are presented

sub-regions roughly divide the Alpine domain according to its major orographic and in particular climatological features (Frei and Schär 1998; Frei and Schmidli 2006; Schär et al. 1998; Schmidli et al. 2002). The southern domain (Alps S) incorporates all regions south of the main crest and is characterized by a strong Mediterranean influence. The region north of the main Alpine crest is split into two sub-domains. The northwestern domain (Alps NW) is characterized by a strong oceanic influence with two annual precipitation peaks; one during winter as a result of low-pressure systems of atlantic origin and one in summer due to convective activity. The northeastern domain (Alps NE) has a pronounced continental character

with largest precipitation amounts due to convective activity during summer. Accompanying analyses for the entire Alpine region as a whole were provided by Gobiet and Kotlarski (2020).

### 2.3 Methods

For each individual model simulation we express future climate change in terms of absolute or relative anomalies of 30-year mean values obtained for the period 2070–2099 with respect to the simulated historical reference period 1981–2010, i.e. as absolute or relative climate change signals. The same reference period is used for transient analyses throughout the twenty-first century. For spatially averaged analyses over the sub-regions Alps NE, Alps NW and Alps S spatial averages over the respective domain are calculated before deriving climate change signals. Model uncertainty is represented by the spread of the analyzed ensemble. This spread arises primarily from the combination of different RCMs with different driving GCMs, but also from the use of different grid spacings (EUR-11 and EUR-44). Moreover, as all driving GCMs provide free-running simulations that are forced by evolving greenhouse gas concentrations only, the analyzed model ensemble can be expected to partly sample internal climate variability as well. This is especially true for the MPI-CSC-REMO2009-MPI-M-MPI-ESM-LR model chain which, for each emission scenario and each grid spacing, provides two simulations based on two different realizations of the driving GCM (see Table S1). Note that, formally, internal climate variability is not a part of model uncertainty as it is not primarily linked to differences among climate models but is triggered by the highly chaotic and non-linear character of the climate system (e.g., Evin et al. 2019; Hawkins and Sutton 2009).

In this work, the best estimate of the change signal for a given parameter and a given emission scenario is represented by the ensemble mean value, model uncertainty ranges are represented by the 5th (q5) and 95th percentile (q95) of the ensemble. Apart from the removal of individual simulations due to general quality issues (see above) we do not carry out any additional model selection or any performance-based model weighting and no model independence assessment (e.g., Knutti et al. 2010; Mendlik and Gobiet 2016; Sanderson et al. 2017). The presented multi-model statistics (mean and uncertainty ranges) have therefore to be considered as first-order sample estimates that do not necessarily reflect the true ensemble statistics. For seasonally stratified analyses the standard climatological seasons are used: DJF (winter, i.e. December to February), MAM (spring, i.e. March to May), JJA (summer, i.e. June to August) and SON (autumn, i.e. September to November). For analyses targeting the elevation dependence of future climate change, elevation band mean values are computed for each individual model

employing the respective model orography before combining model results into a multi-model assessment. For certain analyses only a subset of figures is shown in the main paper (for instance, results for Alps NE), complemented by additional figures in the Supplementary Material (for instance, results for the two remaining sub-regions Alps NW and Alps S). Significance testing (two-sided unpaired t test, p value of 0.05) is carried out for seasonal mean changes of temperature and precipitation over sub-regions. As a complement to the direct analysis of EURO-CORDEX model results for larger domains we also report on results of two case studies in which offline snow models were driven by downscaled and bias-adjusted EUR-11 simulations for the Mont-Blanc massif and the Ötztal Alps (see below).

## 2.4 Case study Mont-Blanc

For an exemplary case study of future snow cover changes in the Mont-Blanc massif (see Fig. 1, lower panel) the downscaling and bias-adjustment method ADAMONT (Verfaillie et al. 2017) employing the SAFRAN reanalysis (Vernay et al. 2022) as a reference meteorological dataset was used to drive the offline snow model Crocus (Vionnet et al. 2012). The entire approach was described by Verfaillie et al. (2018) for one given massif (Chartreuse) and elevation (1500 m), but we here use an expanded number of GCM/RCM pairs (see Table S1) for the Mont-Blanc massif and span a wider range of elevations. The SAFRAN reanalysis provides meteorological fields by steps of 300 m elevation in areas on the order of 1000–1500 km<sup>2</sup> (massifs), assumed to be climatologically homogenous. Meteorological forcing files from both SAFRAN and adjusted climate projections were used as input to the Crocus snow cover model, providing detailed simulations of the evolution of the snowpack, depending on elevation and emission scenario, across the twenty-first century. This approach complements the direct exploitation of EURO-CORDEX simulations in particular because it enables spanning a wider elevation range, and it provides snow cover indicators which are often not computed nor stored in the EURO-CORDEX simulation database. We focus here on the mean winter (November to April) snow depth as an indicator, which is meaningful to many sectors sensitive to the snow cover in the mountain environment. Results are provided in Sect. 6.2 in terms of multi-model average (and standard deviation) of the 15-years multi-annual mean for each GCM/RCM pair for each emission scenario.

## 2.5 Case study Ötztal Alps

A second case study concerning the regional evolution of snow cover characteristics was carried out for the skiing resort Obergurgl in the Ötztal Alps in Tyrol/Austria (see Fig. 1, lower panel). Based on the quantile mapping

approach described in Switanek et al. (2017), an ensemble of EUR-11 simulations (see Table S1 for details) has been bias-adjusted and downscaled for the state territory of Austria (Chimani et al., 2016), based on the datasets SPART ACUS (Hiebl and Frei 2016, 2018) and GPARD1 (Hofstätter et al. 2015). Meteorological forcing from this ensemble of bias-adjusted climate simulations provided input for the snow model SNOWGRID-CL (Olefs et al. 2020) to calculate detailed information of the snow cover at high spatial resolution (1 × 1 km grid or station scale, respectively). In addition, variables relevant for the impact of climate change like runoff from snow melt, or wet-bulb temperature (important for technical snow-making in winter sport resorts) and derived indicators like snow-season length have been provided. In Sect. 6.3 results from this dataset are presented.

## 3 Temperature changes

The past temperature increase in the European Alps (see above) is projected to continue in the course of the twenty-first century. Future changes of regionally averaged mean temperatures depend on the specific emission scenario considered and are, in general, subject to model uncertainty. For the Northeastern Alps (Alps NE) and the strong RCP 8.5 scenario, the ensemble mean increase of annual mean temperature by the end of the century and with respect to the reference 1981–2010 reaches 4 °C (Fig. 2). By contrast, annual mean warming for emission scenarios RCP 2.6 and RCP 4.5 amounts to about 1 °C and 2 °C, respectively. In the former case, the warming is projected to level off around mid-century. The projected mean warming in the individual seasons follows the same general pattern, but is subject to slight seasonal differences. The projected temperature increase is more pronounced in the summer season and is weakest during spring (Fig. 2, lower panels). For Alps NE the end-of-century summer warming is 4.3 °C while warming in spring amounts to 3.1 °C only (Table S2). Autumn and winter are found in between. Similar results are obtained for the two other sub-regions Northwestern Alps (Alps NW; Fig. S1) and Southern Alps (Alps S; Fig S2). However, the projected seasonal mean warming especially for summer and partly also for autumn and spring is more pronounced in Alps S for RCP 4.5 and RCP 8.5 emissions (Table S2). Here, the summer mean temperature increase by the end of the century surpasses 5 °C for RCP 8.5. This stronger warming South of the Alps is part of a well-documented North–South gradient in the projected summer temperature increase across the European continent (Jacob et al. 2014) and probably related to the so-called Mediterranean amplification (Brogli et al. 2019; Kröner et al. 2017).

The projected ensemble mean temperature changes alluded to above can be subject to considerable model

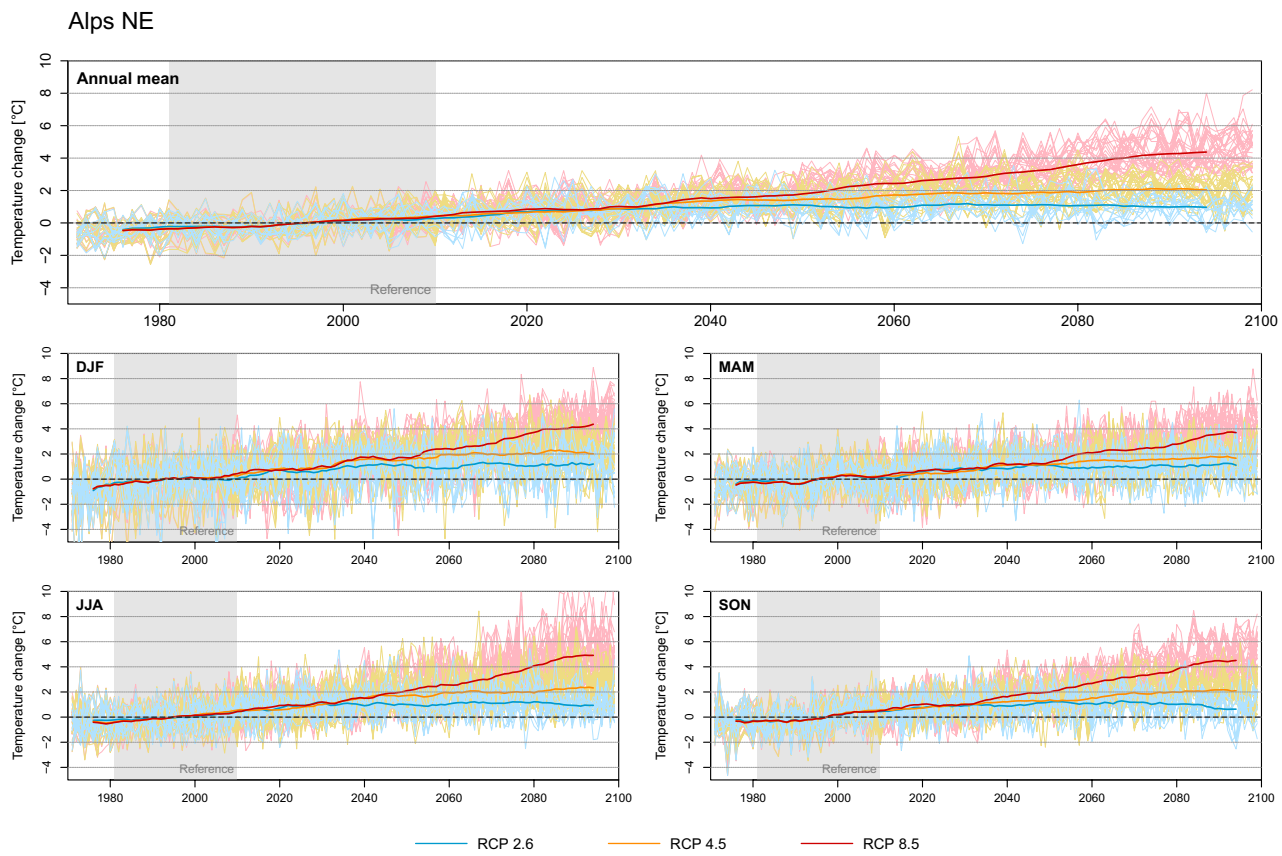


**Fig. 2** Simulated evolution of the mean annual (top) and mean seasonal (bottom) temperature anomaly [°C] with respect to the 1981–2010 mean value and averaged over the Northeastern Alps (Alps NE; see Supplementary Material for the other sub-domains). Line colors

refer to the different emission scenarios. Thin lines denote the individual model simulations of the full ensemble (EUR-11 and EUR-44), bold lines indicate the 11-year running mean of the ensemble mean value

uncertainty, here represented by the ensemble spread (Fig. 3). This spread increases with the strength of the assumed greenhouse gas emissions and the projected mean warming; it is largest for RCP 8.5 and smallest for RCP 2.6. Furthermore, model uncertainty is generally largest for summer. In all sub-domains and for RCP 8.5 the difference between the upper (q95) and the lower (q5) uncertainty estimates for end-of-century summer mean warming is larger than 3 °C. In the case of Alps S, two ensemble members produce a summer mean warming of more than 7 °C by the end of the century (compared to an ensemble mean warming of 5.1 °C). Although these members are found at the far upper end of the ensemble, they have not been excluded due to general quality issues during the ensemble selection process (see Sect. 2.1). A massive summer warming of more than 7 °C in the Southern Alps therefore has to be considered possible in case future greenhouse gas emissions would follow RCP 8.5. Maximum summer temperature increases in the Northeastern and Northwestern Alps are slightly smaller, but are found around 7 °C as well. The projected seasonal mean temperature changes are statistically significant at the

5% level for all RCP 4.5 and all RCP 8.5 model chains (100% of the simulations show a significant change) while, depending on season and sub-region, non-significant changes can arise for RCP 2.6 in up to one third of the simulations (only 67% of the simulations show a significant change in SON for sub-region Alps NE).

The projected warming differences among the three sub-domains already indicate a certain spatial variability of future warming in the Alps. The corresponding patterns of seasonal mean warming by the end of the century are provided by Fig. 4 and Figure S3 for the EUR-11 and the EUR-44 sub-ensemble, respectively. The upper estimate of mean summer warming by the end of the century for RCP 8.5 is larger than 6 °C in each individual EUR-11 grid cell of the analysis domain. Furthermore, in addition to the elevated summer warming in the southern parts of the domain (see above) an amplified warming along the main Alpine ridge becomes apparent, in particular for the higher emission scenarios RCP 4.5 and RCP 8.5. This warming anomaly arises in all four seasons and is evident for the ensemble mean and the upper estimate (q95), and to some extent also for

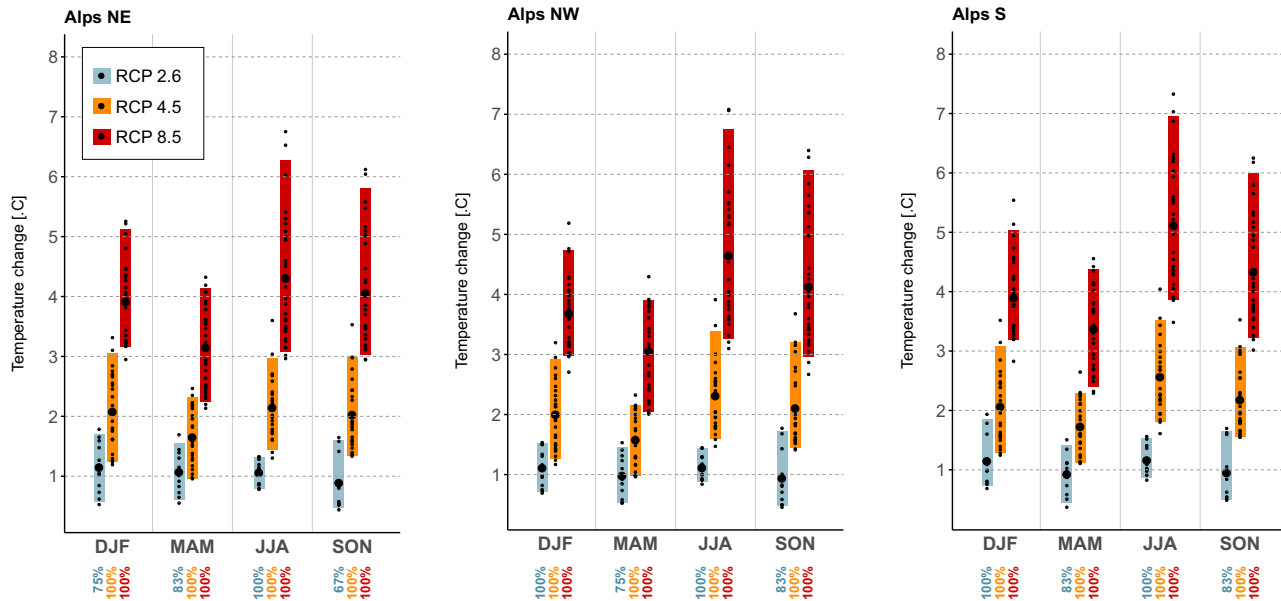


**Fig. 3** Seasonal mean temperature change [ $^{\circ}\text{C}$ ] between 1981–2010 and 2070–2099 in the three sub-domains and for all three emission scenarios considered. Small dots refer to the individual simulations of the full model ensemble (EUR-11 and EUR-44), bold dots to the multi-model ensemble mean. Colored bars indicate the ensemble

uncertainty range as given by the lower (p5) and upper estimate (p95). The numbers below the panels refer to the percentage of simulations (rounded to full numbers) in the respective ensemble that shows a statistically significant change of seasonal mean temperature (two-sided unpaired  $t$  test,  $p$  value of 0.05)

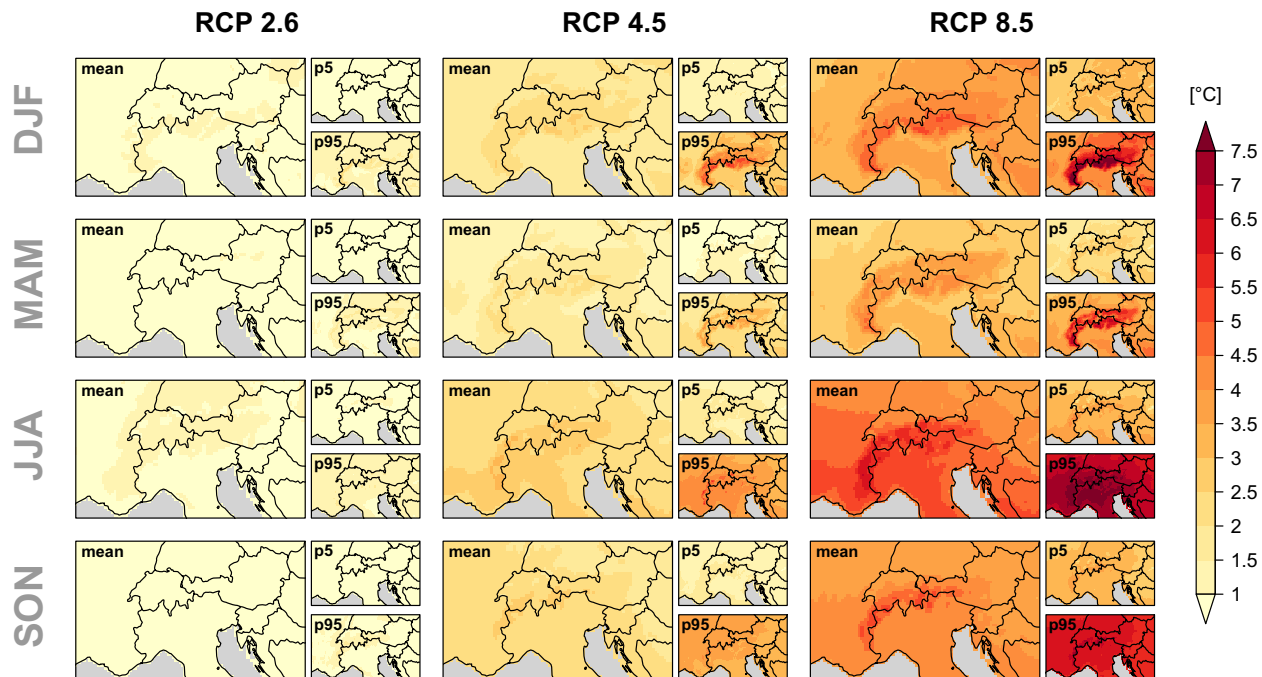


**Fig. 4** Horizontal pattern of the projected seasonal mean temperature change between 1981–2010 and 2070–2099 [ $^{\circ}\text{C}$ ] over the Alpine domain and for the three emission scenarios considered. Columns refer to the individual emission scenarios and lines to the seasons. The large panel of each triple shows the ensemble mean change of the EUR-11 sub-ensemble. The small panels indicate the lower (p5;

upper panel) and upper estimate (p95; lower panel) of the EUR-11 sub-ensemble. Note that mean values and upper and lower estimates have been computed for each grid cell separately and that there is no individual experiment showing these specific patterns. The respective figure for the coarser EUR-44 sub-ensemble is provided in the Supplementary Material (Fig. S3)

the lower estimate (q5). Its basic characteristics are found in both sub-ensembles, although the pattern is partly less evident in the EUR-44 analysis (Fig. S3) where, for instance, mean autumn warming is subject to a minor spatial variability only.

A more detailed picture of this obvious elevation dependency of future warming is provided by Fig. 5 for the EUR-11 sub-ensemble. While the ensemble mean of the projected end-of-century temperature change for the RCP 2.6 emission scenario amounts to about 1 °C for all elevations, changes for RCP 4.5 and RCP 8.5 are subject to a more or less pronounced elevational pattern. Winter and spring maximum warming is found for medium elevations between 1000 and 2000 m and, in the case of RCP 8.5 emissions is about 1 °C larger than warming below 500 m. In summer and autumn the elevation band of maximum warming moves upward and is found above 2000 m with differences. These results are in line with previous works that found similar elevation dependencies of future warming in the Alps and which partly linked this dependency to the snow albedo feedback along the retreating snowline (Gobiet et al. 2014; Kotlarski et al. 2012, 2015).

## 4 Precipitation changes

In contrast to the pronounced and robust change in mean temperature, the EURO-CORDEX climate projections indicate only minor changes in mean annual precipitation sums

for all emission scenarios. Time series are dominated by the comparatively large natural and inter-annual climate variability (Fig. 6 and Figs. S4 and S5). On a seasonal scale, however, distinct trends become apparent from about mid-century except for the autumn season. Characteristic patterns are an increase in wintertime and a decrease in summertime precipitation amounts, with the strengths of these signals scaling with the considered emission scenario. The opposing characteristics of changes in winter and summer precipitation amounts compensate each other at the annual scale, such that overall annual precipitation amounts show no clear signal. Seasonal ensemble mean changes by the end of the century and the associated model spread are shown in Fig. 7. While the magnitude of the climate change signal is obviously a function of the scenario forcing with strong forcing scenarios showing larger change signals, a strong mean signal is in most cases also accompanied by a large model spread. In summer, projected reductions of precipitation amounts are robust for RCP 8.5 emissions with nearly all models projecting reductions up to – 40% in all Alpine sub-domains (ensemble mean signals until the end of the century: Alps NW – 20.8%, Alps NE – 9.0%, Alps S – 17.8%; Table S3). Statistically significant changes at the 5% level are obtained for 36% (Alps NE), 77% (Alps NW) and 65% (Alps S) of the available RCP 8.5 simulations. Conversely, wintertime precipitation increases are prominent with an even more pronounced agreement of simulations towards increasing precipitation amounts across the entire model ensemble. Projected ensemble mean

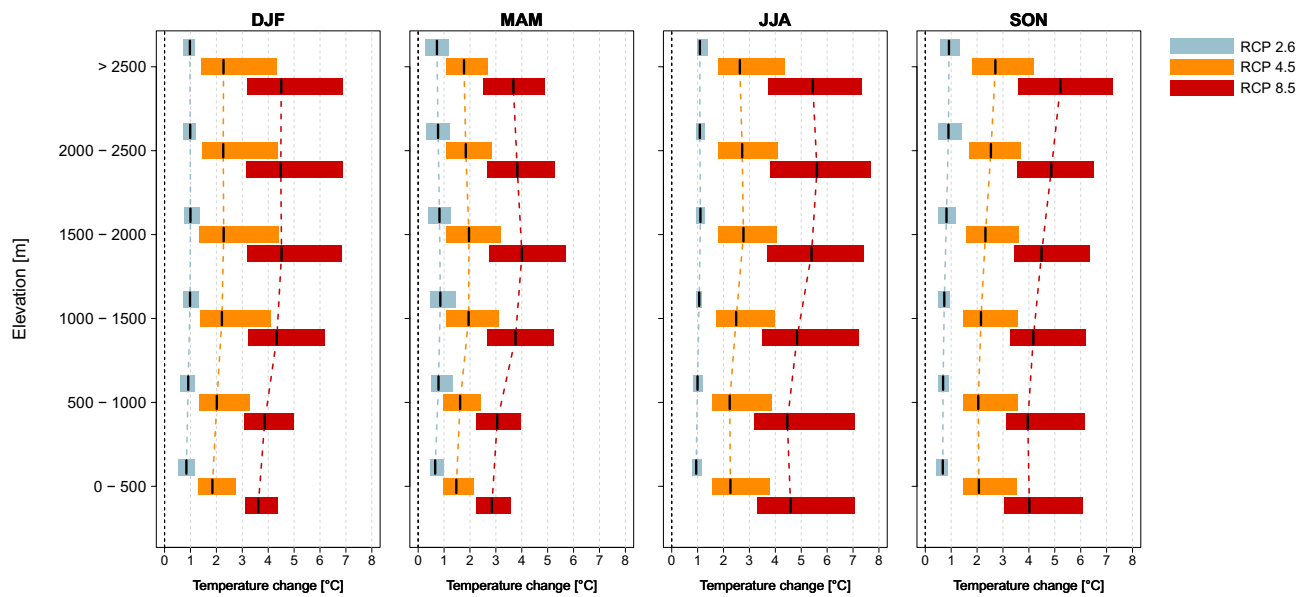


**Fig. 5** Seasonal mean temperature change between 1981–2010 and 2070–2099 [°C] for the three emission scenarios and averaged over 500 m elevation bins (entire Alpine analysis domain). The black vertical lines refer to the ensemble mean change, the bars indicate the

lower (p5) and upper (p95) estimate for each elevation bin. Ensemble mean changes are linearly connected by dashed colored lines. Only the EUR-11 sub-ensemble is used

## Alps NE

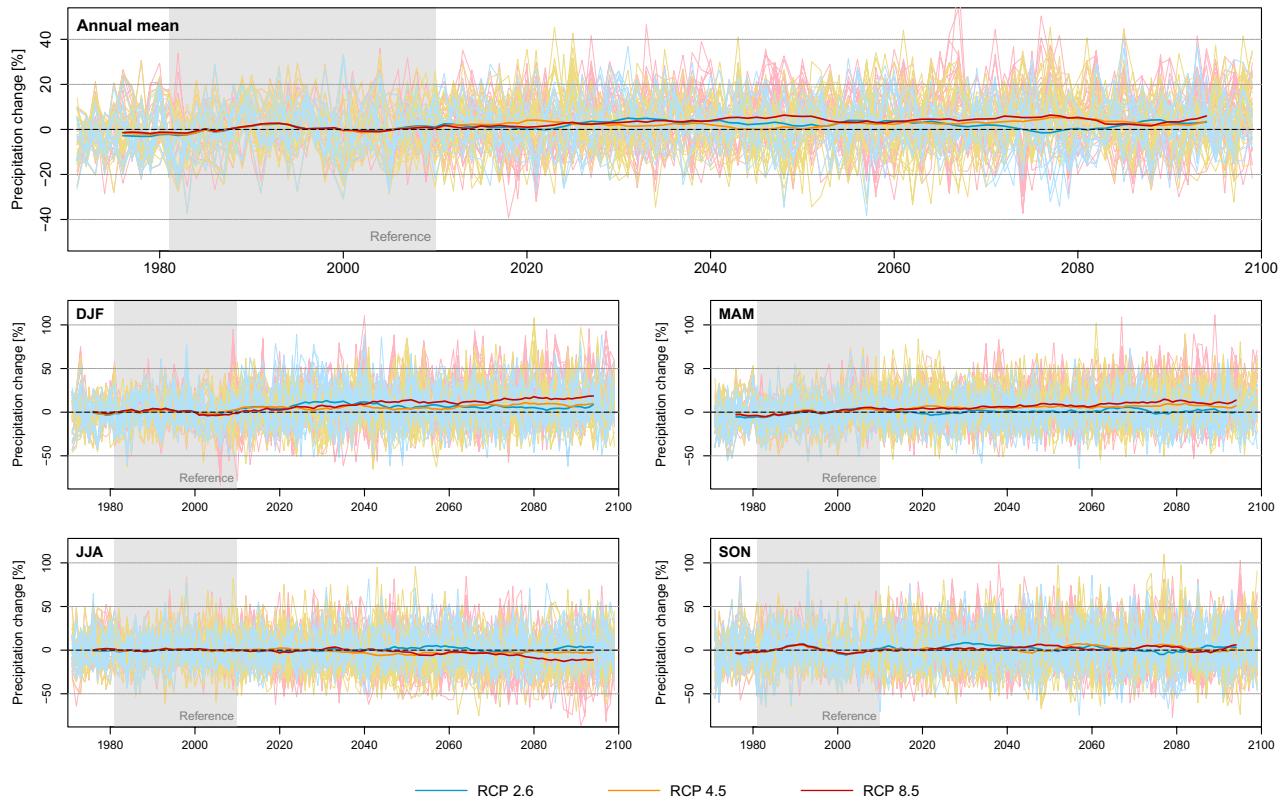


**Fig. 6** Simulated evolution of the mean annual (top) and mean seasonal (bottom) precipitation change [%] with respect to the 1981–2010 mean value and averaged over the Northeastern Alps (Alps NE; see Supplementary Material for the other sub-domains). Line colors

refer to the different emission scenarios. Thin lines denote the individual model simulations of the full ensemble (EUR-11 and EUR-44), bold lines indicate the 11-year running mean of the ensemble mean value

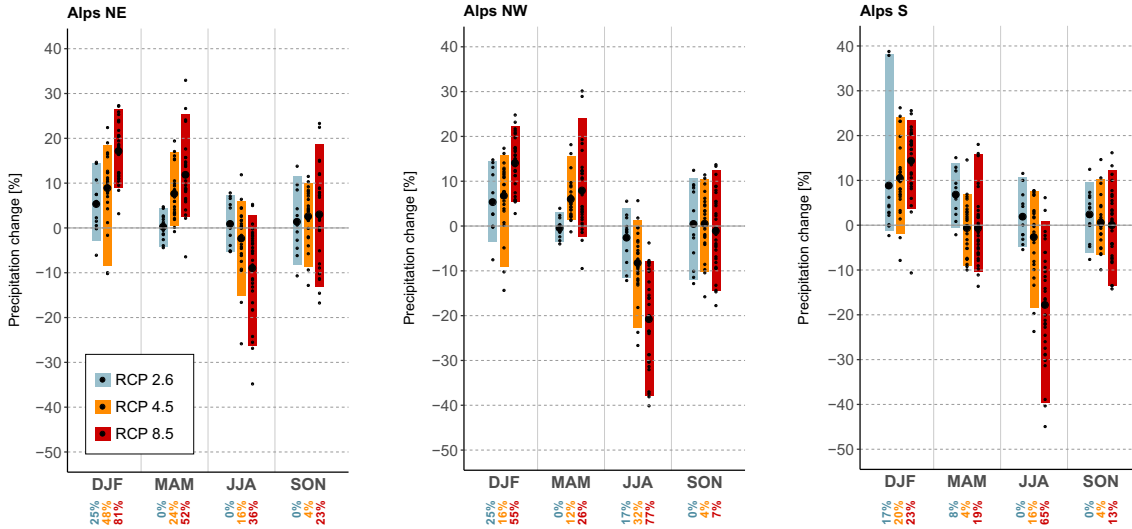


**Fig. 7** Seasonal mean precipitation change [%] between 1981–2010 and 2070–2099 in the three sub-domains and for all three emission scenarios considered. Small dots refer to the individual simulations of the full model ensemble (EUR-11 and EUR-44), bold dots to the multi-model ensemble mean. Colored bars indicate the ensemble

uncertainty range as given by the lower (p5) and upper estimate (p95). The numbers below the panels refer to the percentage of simulations (rounded to full numbers) in the respective ensemble that shows a statistically significant change of seasonal mean precipitation (two-sided unpaired  $t$  test,  $p$  value of 0.05)

wintertime precipitation changes by the end of the century for RCP 8.5 amount to +14.0% (Alps NW), +17.1% (Alps NE) and +14.4% (Alps S; Table S3). The statistical significance of wintertime precipitation changes for RCP 8.5, however, strongly depends on the sub-region with 81% (Alps NE), 55% (Alps NW) and 23% (Alps S) of the simulations showing a statistically significant change. Smaller values are obtained for RCPs 2.6 and 4.5. Climate change signals in the transition seasons tend to lie in between the summer- and wintertime values, with changes in spring resembling a winter-like pattern and signals in autumn being equivocal. The percentage of statistically significant changes in the model ensemble for spring and autumn is mostly smaller than in summer and winter.

The spatial patterns of ensemble-mean precipitation changes by the end of the century for each season and each emission scenario are provided by Fig. 8. Except for RCP 2.6, wintertime ensemble mean precipitation increases are projected for the entire Alpine region, and even more so for the upper change estimate (p95). For RCPs 2.6 and 4.5, however, also a decrease of winter precipitation amounts cannot be ruled out for large parts of the domain according to the lower change estimate (p5). Similar to this but vice versa, summer precipitation decreases become apparent

for most parts of the Alpine domain in the ensemble mean and especially for the lower estimate (p5). In contrast, the upper change estimate (p95) indicates the possibility for an increase of summer precipitation for large parts of the domain and especially for emission scenarios RCP 2.6 and 4.5. In the transition seasons spring and autumn lower change estimates are mostly negative and upper estimates positive with ensemble mean changes being either positive or negative depending on the specific region and the emission scenario considered.

A more detailed insight into the changing character of precipitation is provided by Fig. 9 for the sub-domain Alps NE (Alps NW: Fig. S7, Alps S: Fig S8). It highlights changes in wet-day frequency (fre; an indicator for the future amount of wet days and also an indicator for potential drought risk), wet-day intensity (int; an indicator for the average intensity of wet events at the daily scale) and the maximum daily precipitation amount (rx1d; an indicator for the magnitude of extreme events, such as thunderstorms). It is obvious that the reduction in summertime mean precipitation is driven by a reduction in the number of wet days, while at the same time the wet days intensify. In other words, summer precipitation events become less likely but unfold themselves more intensely if they occur. This indicates that

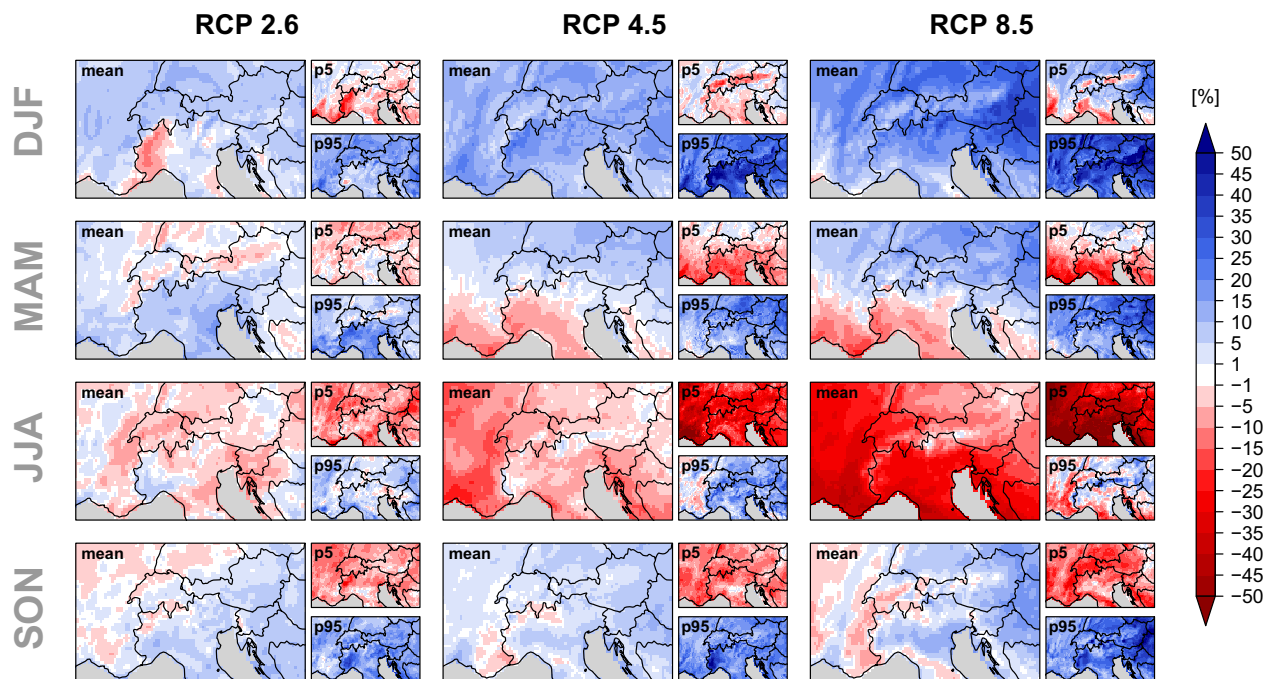


**Fig. 8** Horizontal pattern of the projected seasonal mean precipitation change [%] between 1981–2010 and 2070–2099 over the Alpine domain and for the three emission scenarios considered. Columns refer to the individual emission scenarios and lines to the seasons. The large panel of each triple shows the ensemble mean change of the EUR-11 sub-ensemble. The small panels indicate the lower (p5;

upper panel) and upper estimate (p95; lower panel) of the EUR-11 sub-ensemble. Note that mean values and upper and lower estimates have been computed for each grid cell separately and that there is no individual experiment showing these specific patterns. The respective figure for the coarser EUR-44 sub-ensemble is provided in the Supplementary Material (Fig. S6)

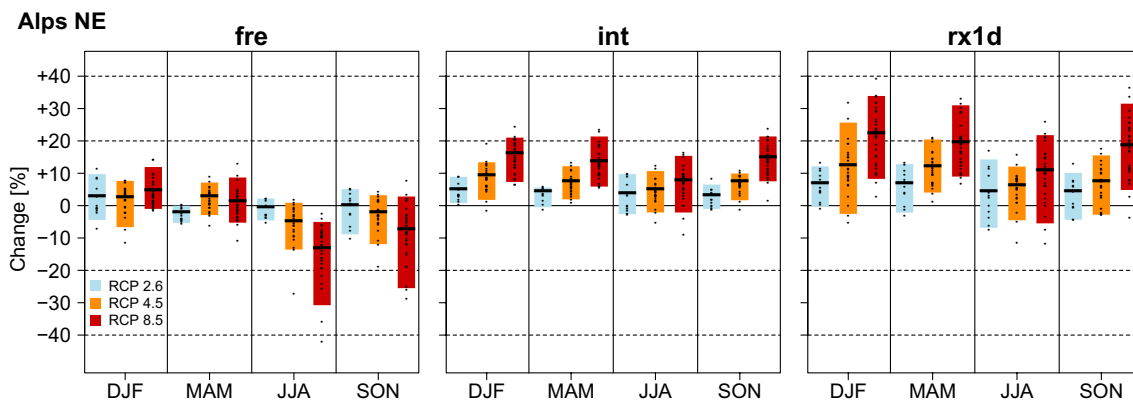


**Fig. 9** Seasonal change in precipitation characteristics [%] between 1981–2010 and 2070–2099 for the Northeastern Alps (Alps NE; see Supplementary Material for the other sub-domains) and for all three emission scenarios considered (color coding). From left to right: wet-day frequency (fre), wet-day intensity (int) and the average maximum

daily event per season (rx1d). Small dots refer to the individual simulations of the full model ensemble (EUR-11 and EUR-44), bold dots to the multi-model ensemble mean. Colored bars indicate the ensemble uncertainty range as given by the lower (p5) and upper estimate (p95)

both kinds of extremes, meteorological droughts and heavy precipitation events, are projected to occur more often in summer under future climatic conditions. In winter, a slight increase in the number of wet days is accompanied by a simultaneous and substantial increase in event intensity and heavy events, leading to the overall increase in wintertime precipitation amounts discussed above. Similar results were obtained by Fischer et al. (2015) for a previous set of Alpine climate scenarios.

It is important to note that heavy precipitation events as represented by int and rx1d do not scale proportionally to changes in seasonal mean precipitation (compare Fig. 7 to Fig. 9). For instance, summer mean precipitation in the Northeastern Alps is projected to decrease by −9% while the projected changes in intensity and the heaviest event per season and year (rx1d) show opposite signals with +7% and +10% (RCP 8.5). In wintertime a simple disproportionality appears with a signal of +17% for the mean and +21% for the heaviest event (rx1d). In this context, an in-depth analysis on changes in extreme precipitation in the EURO-CORDEX model ensemble indicates significant increases that come along with distinct reductions in the return periods of heavy events across the entire Alpine region (Rajczak and Schär 2017).

## 5 Combined temperature and precipitation changes

Future changes in temperature and precipitation can be assumed to partly depend on each other as, especially at regional scale, both variables are strongly inter-linked via the nature of the impinging air masses and regional-scale feedback mechanisms. Hence, for specific applications the

uncertainty ranges for temperature and precipitation change presented above can not necessarily be freely combined with each other but have to be assessed in combination. Such a combined assessment offers the ability to analyze multivariate or compound impacts, to study driving processes and allows to select appropriate model chains or scaling parameters that support storyline-based analyses of future climate change impacts.

For Switzerland and based on a previous RCM ensemble of the ENSEMBLES project (van der Linden and Mitchell 2009), Fischer et al. (2016) found a pronounced negative correlation between projected seasonal mean temperature and precipitation changes in the summer season, but a much weaker relation in the other seasons. These results are largely confirmed when analyzing the EURO-CORDEX ensemble (Fig. 10). A strong negative relation between both indicators is obtained in all sub-domains, i.e., summer precipitation amounts decrease as a function of the projected warming. This relation is apparent especially within members of the high-end RCP 8.5 emission scenario, but also between emission scenarios; summer precipitation decreases are stronger for RCP 8.5 than for RCPs 4.5 and 2.6. Note that this relation holds for seasonal mean changes only and despite the thermodynamic intensification of short term summer precipitation amounts (Sect. 4). This possibly indicates a strong influence of large scale dynamics that overcompensates a regional-scale thermodynamic influence on shorter time scales. At least for the southern part of the Alps, which are considerably influenced by the Mediterranean climate, this hypothesis is backed by Brogli et al. (2019) who found future Mediterranean summer drying to be strongly connected to meridional temperature change gradients that are partly driven by circulation changes. The tendency for an amplified summer drying signal with an increasing summer

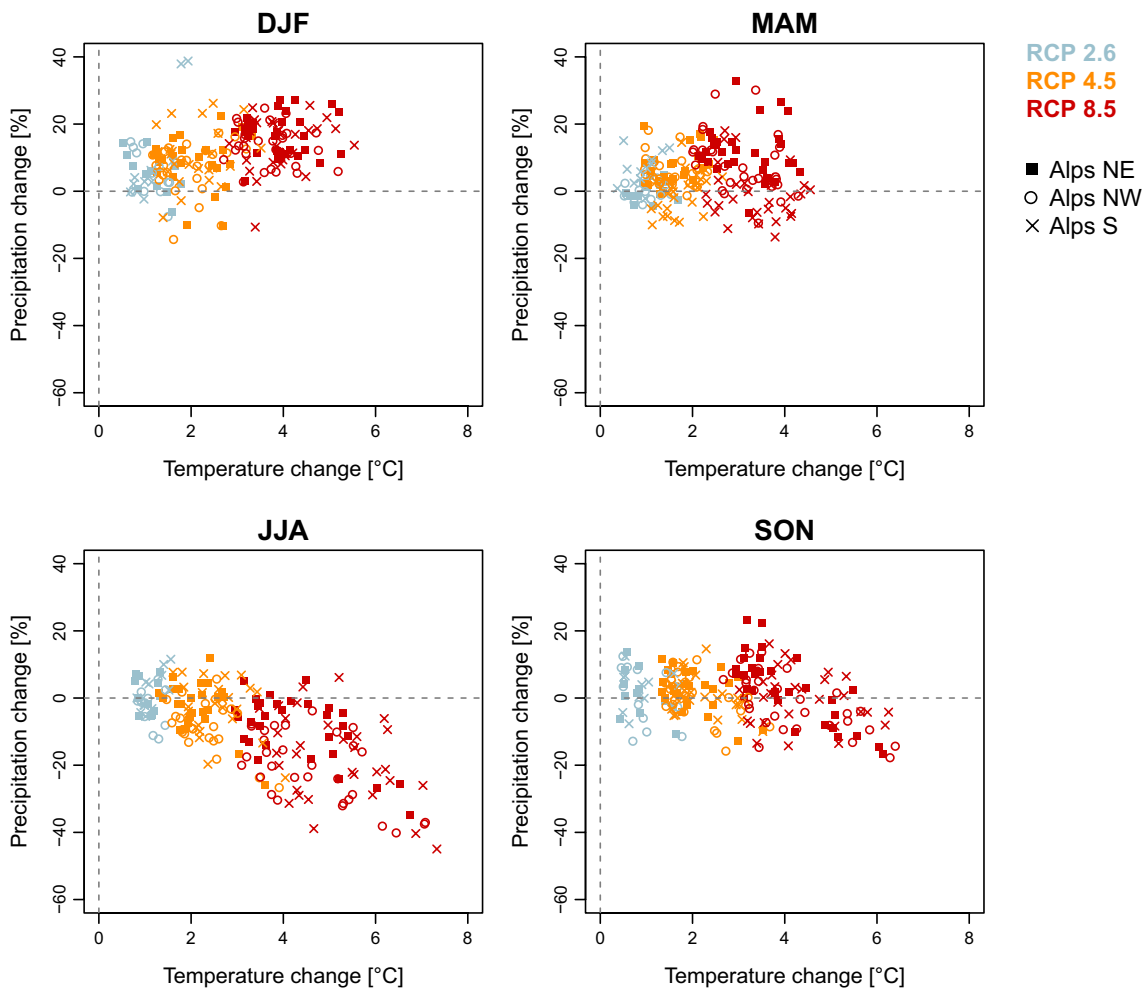


**Fig. 10** Relation between mean seasonal temperature (x-axis) [°C] and precipitation changes (y-axis) [%] in the Alpine region from 1981–2010 to 2070–2099, for all experiments of the full multi-model

ensemble (EUR-11 and EUR-44). The four panels represent the individual seasons, the colors indicate the three different emission scenarios. The marker styles refer to the three Alpine sub-domains

warming is also consistent with past observations which, at least for individual regions, reveal decreasing summer precipitation sums during the past decades that were subject to a pronounced summer warming (Scherrer et al. 2022).

In contrast to summer, wintertime temperature and precipitation changes are positively correlated; in all sub-domains a stronger winter warming implies larger relative increases of precipitation. The relation is, however, less pronounced compared to summer. It becomes apparent only when comparing signals for the different emission scenarios to each other and can hardly be identified within the individual emission scenarios. Reasons for the weak positive relation might be the increase of the moisture holding capacity in air masses advected towards the Alps and an increased specific humidity associated with a general increase of precipitation amounts (Allen and Ingram 2002; Soden et al. 2005). Again, these results are consistent with historical observations that indicate increasing winter precipitation

amounts with ongoing warming especially North of the Alps (e.g. CH2018 2018). The transition seasons autumn and spring show no clear relation between the projected temperature and precipitation changes, except for a slight tendency for decreasing autumn precipitation in experiments with very strong warming.

## 6 Snow cover changes

### 6.1 Alpine scale

Snow cover is an important natural resource in the European Alps and a diverse range of sectors such as winter tourism, hydropower generation, water resources management, civil defence, public traffic and ecology heavily depend on the presence of natural snow (Hock et al. 2019, Adler et al. 2022). Moreover, snow is an interactive agent in the Alpine

climate system due to its modulation of surface-atmosphere exchange processes (Armstrong and Brun 2008). The prevailing climatic forcing influences the presence of surface snow cover in several ways, most importantly via its control on snow accumulation (snowfall) and snow ablation (snow melt). Regarding the former, the projected temperature and precipitation changes presented above can be thought to have opposing effects on mean snowfall sums. First, a projected increase of mean temperature will be associated with a decrease in the snowfall fraction (the contribution of snowfall to total precipitation) and a corresponding increase in the rainfall fraction (the contribution of rainfall to total precipitation). In the absence of any total precipitation changes, this would lead to an overall reduction in snowfall sums (total accumulated snowfall). Second, the tendency for increases in total wintertime precipitation (see Sect. 4) might partially offset this temperature effect and lead to higher snowfall sums compared to a non-modified precipitation regime. Previous studies on past and future snowfall changes in the Alps indicate a dominance of the temperature effect and project substantial snowfall reductions (de Vries et al. 2013, 2014; Piazza et al. 2014; Serquet et al. 2011), though not explicitly targeting very high elevations due to the coarse resolution of the underlying models. A more comprehensive analysis specifically targeting the European Alps and employing a EURO-CORDEX sub-ensemble has recently been presented by Frei et al. (2018). The authors find a robust future decrease of winter snowfall amounts over most parts of the Alps with domain-mean decreases by the end of the century of about – 25% and – 45% for RCPs 4.5 and 8.5, respectively. These snowfall reductions are primarily driven by the projected warming and are connected to an important decrease of both snowfall frequency and snowfall fraction.

A direct consequence of the expected widespread decrease of Alpine snowfall sums is a reduced snow accumulation at the surface. Furthermore, rising temperatures can be expected to accelerate the melt process and thus the ablation of the surface snowpack. We here analyse projected future changes of the water equivalent of the snowpack

(SWE) as directly simulated by the land surface schemes of the EURO-CORDEX RCMs. Note that, compared to the application of offline snow cover models, such an analysis ensures a full consistency between the simulated changes in the snowpack and its atmospheric drivers. However, it requires special care due to the simple nature of the snow parameterization schemes embedded in climate models and due to the fact that simulated snow cover amounts are typically not comprehensively evaluated during climate model development and calibration (Steger et al. 2013).

The geographical pattern of projected mean September-May SWE changes until the end of the century shows an overall decrease that is clearly controlled by elevation (Fig. 11). For the low-end RCP 2.6 emission scenario, large SWE losses are restricted to the Alpine forelands while regions along the main Alpine ridge are projected to experience only small decreases or even no SWE change at all. Slight positive signals are obtained for snow-sparse regions south of the Alps which is presumably related to their very infrequent snow coverage even in today's climate and largely associated with internal climate variability (note that the RCP 2.6 ensemble employed for the snow cover analysis consists of two simulations only). For RCP4.5, SWE reductions of more than 50% are projected for large regions north and south of the main Alpine ridge. In particular, low-lying areas in northern Italy (Po valley) and southeastern France are affected by SWE losses exceeding 80%. Changes at medium to high elevations along the main Alpine ridge are less pronounced and typically do not exceed 30%. In contrast, SWE losses of more than 50% are obtained at medium to high elevations for RCP 8.5. For this scenario large parts of the Alpine forelands are projected to experience SWE reductions of more than 80%, up to almost complete losses in the Po valley south of the Alps and in parts of southeastern France.

A clearer picture of the apparent elevation dependency of the projected mean SWE changes in the Alps by the end of the century is provided by Fig. 12. For all three emission scenarios, relative SWE losses are most pronounced at elevations below 1000 m a.s.l. Note that change signals for RCP

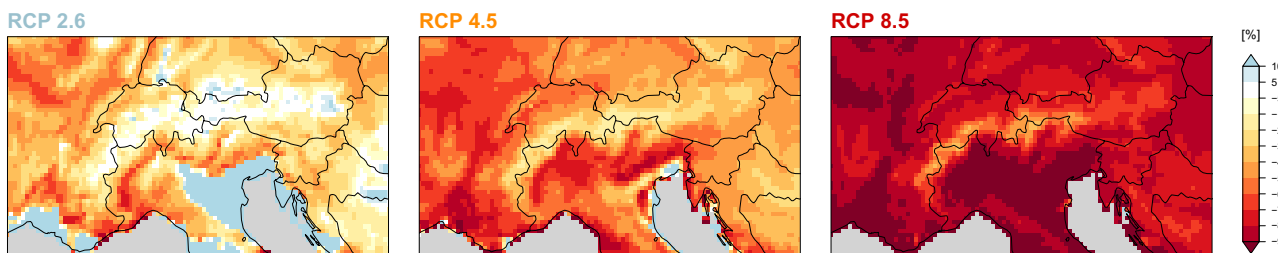


**Fig. 11** Projected change of the mean September to May snow water equivalent in the Alpine region from 1981–2010 to 2070–2099 [%] for the three emission scenarios. Values refer to the ensemble mean

change of the reduced EUR-11 sub-ensemble employed for the snow cover analysis (see Table S1)

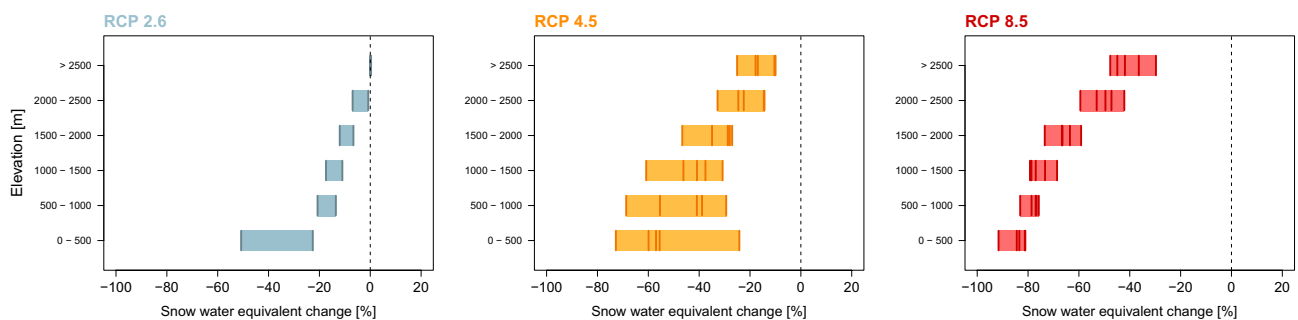


**Fig. 12** Projected change of the mean September to May snow water equivalent in the combined Alpine analysis domain (see Fig. 1) from 1981–2010 to 2070–2099 [%] for the three emission scenarios and for individual elevation bands. Vertical lines refer to the mean SWE

change in the respective elevation band in each individual member of the reduced EUR-11 sub-ensemble employed for the snow cover analysis (see Table S1). Colored bars indicate the full multi-model range

2.6 should be treated with care since they are based on two simulations only. For this low-end emission scenario reductions of SWE of less than 20% are obtained for elevations above 500 m and losses between 20 and 50% for lower elevations. In the case of RCP4.5, a considerable model spread of change signals is found below 500 m, with elevation-mean losses ranging from about 25 to 80%. The upper end of this range ( $-25\%$ ) is, however, based on a model simulation that considerably diverts from the bulk of the ensemble and represents a clear outlier. At higher reaches, relative SWE losses for RCP 4.5 are becoming smaller and amount to  $-10$  to  $-30\%$  for regions above 2500 m. In case of high-end RCP 8.5 emissions, all models agree on substantial SWE losses between about 80 and 90% at elevations below 500 m. Moving upward, relative SWE losses become less pronounced but are still substantial. SWE at elevations above 2500 m is projected to decrease by about 30–50%.

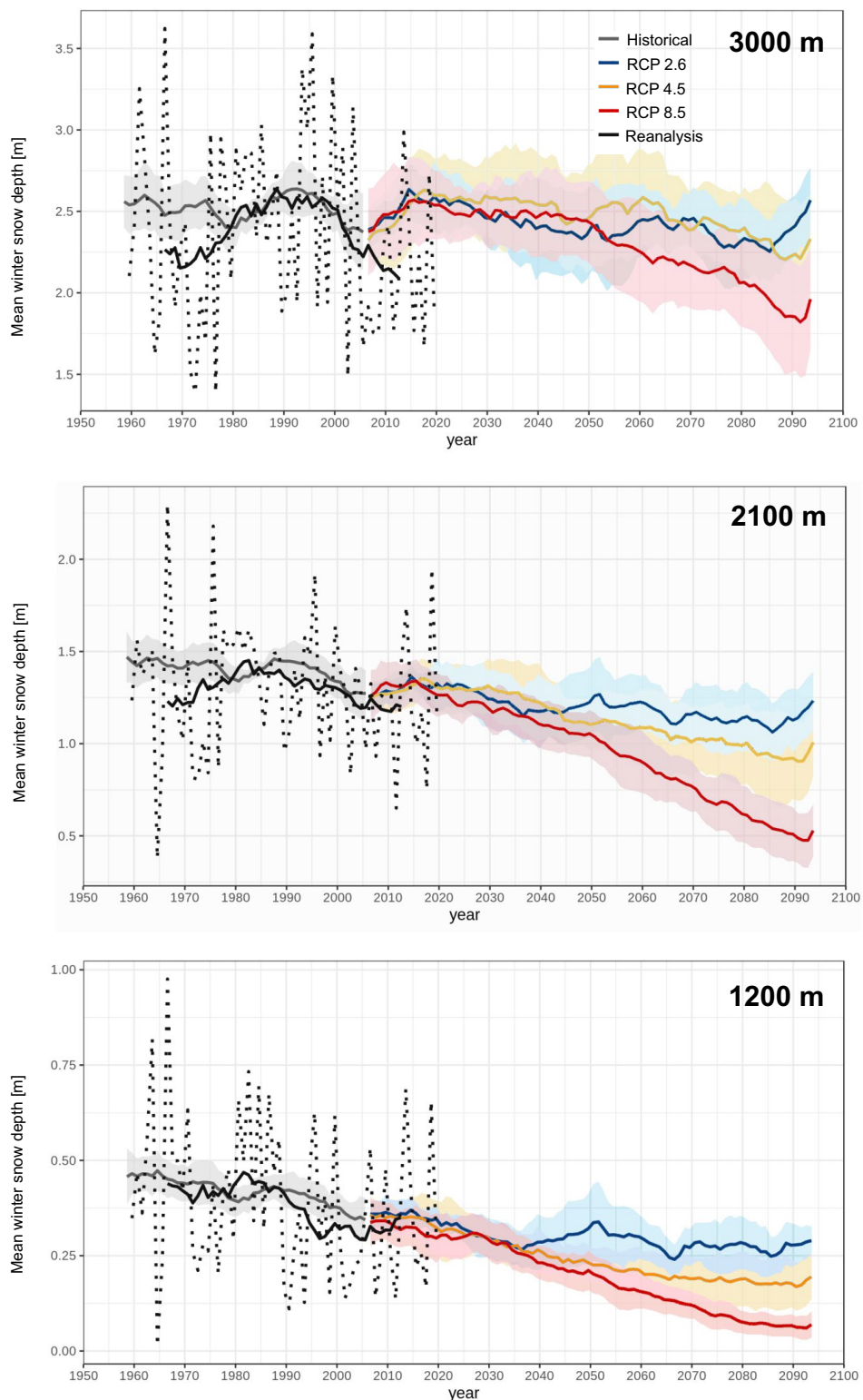
## 6.2 Mont-Blanc

Specific results for snow cover changes in the Mont-Blanc area are provided in Fig. 13, based on the bias adjustment and downscaling method described in Sect. 2.4, followed by dedicated snow cover model runs using the adjusted EURO-CORDEX climate change projections. The figure provides results at 1200, 2100 and 3000 m elevation, representative of typical environments within a given mountain range. The evolution of the mean winter snow depth in climate projections across the period from 1950 to 2100 is superimposed by annual values of the mean winter snow depth from the SAFRAN-Crocus reanalysis from 1958 to 2019. The fluctuations of the annual values of the reanalysis-based snow depth strongly exceed, below and above, the multi-model mean and standard deviation of multi-annual average values. This highlights the strong interannual variability of the mountain snow cover at all elevations, under past and current climate, which is often masked out using multi-model

and multi-annual means. In addition to the strong interannual variability, the reanalysis shows a strong decreasing trend, more substantial at lower elevation (1200 m) than higher up (2100 m) and not detected at 3000 m elevation, consistent with the latest assessments of snow cover trends in the Alpine region (Matiu et al. 2021). Projections into the twenty-first century show a decrease of mean winter snow depth for all scenarios and lower elevations until mid-century. Compared to the beginning of the century, for the 15-years period centered on 2040, the mean winter snow depth at 1200 m is projected to decrease from 0.4 m to 0.25 m (decrease of the order of 30%), at 2100 m from 1.4 m to 1.2 m ( $-15\%$  approximately). About 2.5 m of snow depth remains at 3000 m. Across the scenarios used, for the second half of the twenty-first century, the mean winter snow depth values for RCP 2.6 remain on the order of the value reached in mid-century. For RCP 4.5 and RCP 8.5, the decrease continues throughout the twenty-first century in projections, with stronger decreases for RCP 8.5, including decreases at 3000 m elevation. There, the multi-annual multi-model mean winter snow cover values drop below 2 m ( $-25\%$ ) for RCP 8.5 at the end of the century, with even more substantial decreases at 1200 m, reaching 0.2 m ( $-50\%$ ) for RCP 4.5 and 0.1 m ( $-75\%$ ) for RCP 8.5. Such low values indicate that snow free winter seasons will become increasingly frequent throughout the second half of the century. At 2100 m, the mean winter snow depth multi-annual multi-model mean values reach values below 1 m for RCP 4.5 ( $-30\%$ ) and 0.5 m ( $-65\%$ ) for RCP 8.5. Note that this can be interpreted as a shift corresponding to approximately 1000 m elevation, i.e. the end of century RCP 8.5 snow cover state is comparable to the snow cover state at 1200 m elevation at the beginning of the century.

Although several post-processing steps involving statistical adjustments and running an offline snow cover model are involved, the results of this case study are highly consistent with the analysis of the EURO-CORDEX raw

**Fig. 13** Snow cover changes in the Mont-Blanc region at three elevations (3000 m, 2100 m and 1200 m above mean sea level), from 1950 to 2100. The dotted line corresponds to annual values of the mean winter (Nov.-Apr.) snow depth. The black continuous line shows the corresponding 15-years moving average. Grey (historical) and colored (future projections) lines correspond to the multi-model mean (surrounded by 1 standard deviation) of 15-years multi-annual values from all available GCM/RCM pairs for each RCP



simulations. However, there is specific added value in this approach, because it enables spanning a wider elevation range, including elevations above the highest point of the EURO-CORDEX model topography. This makes it possible to more directly feed mountain-related impact models

for applications in the field of water resources or glacier mass balance (e.g. Peyaud et al., 2020). Furthermore, this approach provides access to snow-related indicators which are not typically included in EURO-CORDEX RCM output. While this is demonstrated here using mean winter snow

depth, further indicators can be computed, and the adjusted meteorological forcing files can be used for specific configurations of the Crocus snow cover model e.g. including snow management including grooming and snowmaking, highly relevant for ski tourism climate change impact studies (e.g. Spandre et al., 2019). Overall, this example shows the strong consistency between the EURO-CORDEX models output, and refined downstream applications of the models, thereby providing confidence in the ability of these methods to provide complementary and coherent information for various scales of application.

### 6.3 Ötztal Alps

Specific results for the Ötztal Alps case study are shown in Fig. 14. These results are part of a more comprehensive study that assesses future snow cover changes for the skiing resort Obergurgl. Here we only regard the natural snow cover, since effects of technical snow production are out of the scope of this paper, but further details can be found in Koch et al. (2020a). In addition, a comprehensive overview on trends in past snow cover in Austria is given in Olefs et al. (2020).

Near the valley station of this high-altitude skiing resort at 1920 m a.s.l. at a 15° Northwest-facing slope, the mean snow season length (number of days with at least 30 cm snow depth between November and April, Fig. 14, lower panel) is characterized by large inter-annual variability, superimposed onto a clear negative trend. The climate scenarios project a further decline of snow season length until 2050 with a loss of about 40% compared to the period 1971–2000 in all RCPs. After 2050, snow cover stabilizes in the RCP 2.6 scenario, while the trend continues for RCP 4.5 and RCP 8.5. In the high-end RCP 8.5 scenario, the loss amounts to more than 80% at the end of the twenty-first century. Figure 14 (upper panel) also shows the same indicator for a 20° Northwest-facing slope at 2500 m a.s.l. In this case, no significant trend can be found in the past period, and the losses until 2050 are limited to about 10% for all emission scenarios, followed by a stabilization for RCP 2.6 and RCP 4.5 and a further decrease until about—35% in 2100 for RCP 8.5. It has to be noted, that these results only refer to specific altitude levels and slope orientations. More examples with further altitudes and orientations are provided by Koch et al. (2020a, b). Similar to the Mont Blanc study presented in Sect. 6.2, the Ötztal case study presents an example

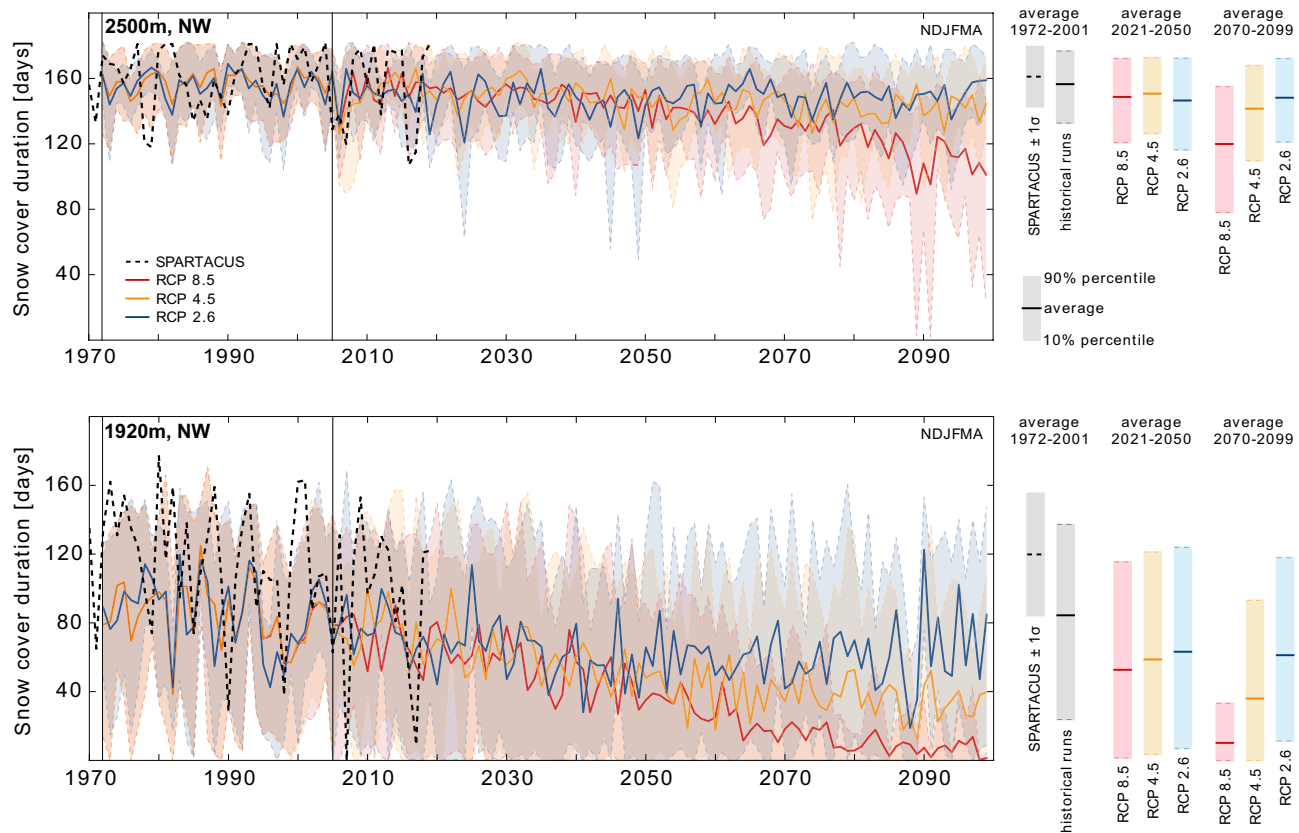


**Fig. 14** Number of days per winter (November–April) with snow depth > 30 cm at two Northwest-facing slopes in the Ötztal Alps at 2500 (upper panel) and 1920 m a.s.l (lower panel) as simulated by

the SNOWGRID-CL model when driven by observation-based meteorological forcing (SPARTACUS) and by the bias-adjusted EUR-11 sub-ensemble

for a refined local analysis based on a bias adjustment and further downscaling of the EURO-CORDEX model output and the offline forcing of a dedicated model of the surface snow pack. Again, the results obtained are largely consistent with the RCM-based snow cover analysis, but allow for a refined and locally more meaningful assessment of future snow cover changes.

## 7 Discussion

The results presented in the previous sections provide a detailed picture on how the climate of the European Alps might change throughout the twenty-first century. By and large, they confirm previous studies and previous assessments that were based on either older climate model ensembles originating from the PRUDENCE (Christensen and Christensen 2007) and ENSEMBLES (van der Linden and Mitchell 2009) projects or smaller ensembles already originating from the current EURO-CORDEX initiative. Note that a fully consistent quantitative comparison is hindered by the different underlying greenhouse gas scenarios employed in previous assessments. Most importantly, our results are qualitatively in line with the previous ENSEMBLES-based assessment of future Alpine climate change presented by Gobiet et al. (2014). However, the larger ensemble size of the EURO-CORDEX ensemble used in the present work and the comparatively high spatial resolution of the EUR-11 sub-ensemble allow a spatially more explicit assessment and a more decent quantification of intrinsic projection uncertainties.

Regarding the projected temperature change, we obtain an unequivocal and robust signal of future warming in the entire Alpine region for all seasons. The general magnitude of this warming is largely driven by the underlying emission scenario with the strongest warming projected for the high RCP 8.5 scenario. On a seasonal scale, the projected temperature increase is slightly higher in summer compared to the other seasons. The reason for this differential warming throughout the annual cycle might partly be related to soil moisture-atmosphere feedbacks following an overall summer drying (see below; e.g. Seneviratne et al. 2010) but might also involve changes of large-scale circulation patterns and changes in vertical atmospheric stability (Kröner et al. 2017). Previous studies have shown that the summer mean warming over many parts of Europe including the Alps and especially the increase of hot temperature extremes of the EURO-CORDEX RCMs is systematically smaller than the warming in their driving GCMs. This feature can partly be attributed to the missing representation of plant physiological responses and the absence of time-varying anthropogenic aerosol concentrations in most regional simulations (Boé et al. 2020; Schwingshackl et al. 2019). Still and despite

these missing elements, Sørland et al. (2018) have shown that the EURO-CORDEX RCMs tend to reduce biases of their driving GCMs even on larger scales that are well resolved by global models, providing a certain degree of confidence in the ability of the EURO-CORDEX RCMs to also properly represent future change signals. Regarding the spatial pattern of the simulated warming over the Alpine region, we find an obviously elevation-driven variability in the EURO-CORDEX ensemble with a maximum warming at medium (winter, spring) and high (summer, autumn) elevations. These results are consistent with previous works (Gobiet et al. 2014; Kotlarski et al. 2012, 2015; Warscher et al. 2019), but are at least to some extent inconsistent with observed evidence (Rottler et al. 2019). This might be related to an overestimated sensitivity of RCM-simulated near-surface temperature conditions to the presence or absence of snow, possibly exaggerating the local snow-albedo feedback (Winter et al. 2017). Furthermore, trends in concentrations of anthropogenic aerosols have been identified as possible drivers of elevation-dependent temperature changes (Rangwala and Miller 2012; Mountain Research Initiative EDW Working Group 2015) but are to a large extent neglected in the EURO-CORDEX simulations (Boé et al. 2020). Also note that observed elevation dependencies of Alpine warming are subject to a large variability owing to the multitude of potential processes involved (Kuhn and Olefs 2020). Still, many mountain regions around the globe have shown a tendency toward enhanced warming at high elevations (Pepin et al. 2022).

In contrast to temperature, projected changes in mean precipitation are characterized by no clear change signal at the annual scale but a notable redistribution of precipitation between seasons. This is reflected by increases in winter and decreases in summer precipitation amounts and is connected to continental scale precipitation change patterns. Previous works already revealed that the Alpine region is located within a seasonally oscillating transition zone separating precipitation increases in the north of Europe from decreases in the south (Rajczak and Schär 2017). This zone is located across northern Europe in summer and the Mediterranean region in winter, with the Alpine region being located either north (winter) or south (summer) of it. As for temperature, the magnitude of the projected precipitation changes strongly depends on the scenario forcing, with weaker signals for RCP 2.6 and stronger signals for RCP 8.5. However, strong changes in mean seasonal precipitation tend to emerge only after the second half of the twenty-first century. A prominent feature of the projected precipitation change is its disproportionate behavior in terms of changes in mean precipitation as compared to changes in heavy and extreme precipitation. These do not scale proportionately or even show opposite signs of change (Ban et al. 2020; Frei and Schmidli 2006; Rajczak et al. 2013;

Rajczak and Schär 2017). In summer, for instance, heavy events are projected to intensify while mean amounts are subject to a decrease. Changes found in heavy precipitation also tend to show up much clearer than changes in the mean, which is also already reflected in observations from recent decades (Schmidli and Frei 2005; Scherrer et al. 2016). In general, projected changes in precipitation as simulated by the EURO-CORDEX simulations are largely consistent with projections from the ENSEMBLES and PRUDENCE initiatives. Some obvious differences appear in the transition seasons when the exact position of the seasonally dependent transition zone, separating increasing precipitation amounts in the north from decreasing amounts in the south, is particularly uncertain. Differences between the EURO-CORDEX and the previous ENSEMBLES RCM ensemble are therefore found in autumn, for which ENSEMBLES showed pronounced increases in precipitation amounts in the Alps (Rajczak et al. 2013) while EURO-CORDEX shows small or equivocal changes in autumn and particularly increasing magnitudes in winter (Fig. 7; Rajczak and Schär 2017). Also, the new EURO-CORDEX ensemble is subject to slightly larger model uncertainty in summer precipitation change, which might be linked to the increased number of considered models.

The results presented here focus on daily and seasonal precipitation statistics. Certain natural hazards such as small-scale catchment flooding events, however, are highly sensitive to events that occur at the sub-daily (e.g. hourly) timescale. Capturing such events requires computationally expensive simulations at the kilometer-scale, also called convection-permitting or convection-resolving climate simulations (Lucas-Picher et al. 2021; Prein et al. 2015, 2020; Schär et al. 2020). Up to now, such simulations have mostly been carried out in pioneering studies using single models for very limited areas (Kendon et al. 2017; Prein et al. 2015) and ensemble information from respective models only recently became available (e.g. Ban et al. 2021; Coppola et al. 2020; Pichelli et al. 2021). For the Alpine region, first experiments provide valuable insights in terms of the capability of such high-resolution simulations to better represent heavy precipitation characteristics and their future changes especially at sub-daily timescale compared to the coarse-resolved ensembles exploited in the present work (Ban et al. 2015, 2020, 2021). Further, added value of convection-permitting model simulations that is not yet exploited in the EURO-CORDEX ensemble analyzed here can be expected in terms of very high elevation climate change, climate change in complex topography and changes of small-scale extreme weather events. Lüthi et al. (2019) furthermore reveal the potential of convection-permitting simulations to better represent high elevation snow cover changes. Regarding the latter, the evaluation exercise carried out in CH2018 (2018; see Sect. 2.1) and the previous work

of Steger et al. (2013) show that climate-model simulated snow cover has to be treated with special care and requires a careful evaluation of simulations before using them to assess future change signals. If done so, the available ensemble clearly shows that the effect of the projected temperature increase dominates possible winter precipitation increases in terms of SWE changes. This is consistent with the snowfall analysis of Frei et al. (2018). Except for very high elevations, important SWE reductions are to be expected for all emission scenarios. Largest percentage decreases up to an almost complete loss of surface snow cover are obtained for low elevations and for the high-end RCP 8.5 scenario. Dedicated regional analyses employing offline snow models such as those presented for the Mont-Blanc region and the Ötztal Alps are largely in line with the climate model-based assessment, but allow for a much more detailed and site-specific analysis of changes in individual snow indicators.

## 8 Conclusions

We here present a comprehensive analysis of projected twenty-first century Alpine climate change based on the regional climate simulation database of the EURO-CORDEX initiative. The core simulation ensemble has been subject to a dedicated evaluation exercise carried out in the frame of the CH2018 Climate Scenarios for Switzerland (CH2018 2018). The results obtained largely agree with previous works based on older generations of RCM ensembles. However, due to the comparatively large ensemble size and the high spatial resolution, the employed EURO-CORDEX ensemble allows for a more decent assessment of inherent projection uncertainties and of spatial details of future Alpine climate change.

Overall, the entire Alpine region will face a warmer climate in the course of the twenty-first century for all emission scenarios considered. The strongest warming is projected for the summer season, for regions south of the main Alpine ridge and for the high-end RCP 8.5 emission scenario. Depending on the season, the warming will be slightly enhanced at medium to high elevations. Model uncertainty can be considerable, but the major warming patterns are consistent across the ensemble. For the case of precipitation, the bulk of the ensemble agrees on a seasonal shift of precipitation amounts characterized by precipitation increases in winter and by decreases in summer over most parts of the analysis domain. However, model uncertainty is generally higher and individual simulations can show change signals of opposite sign. Daily precipitation intensity is projected to increase in all seasons and all sub-domains, while the wet-day frequency will decrease in the summer season. The projected temperature change in summer (winter) is negatively (positively) correlated with

the precipitation change, i.e., simulations and/or regions with a strong seasonal mean warming typically show a stronger precipitation decrease (increase). In general and for all indicators, the magnitude of the change signals increases with the assumed greenhouse gas forcing, i.e., is smallest for RCP 2.6 and largest for RCP 8.5 with RCP 4.5 being located in between.

The consequences of the described changes of the Alpine climate will be manifold and will concern a large number of dependent natural and anthropogenic systems. Among these is the Alpine cryosphere, characterized by snow, glacier ice and permafrost. In an exemplary expansion of our analysis to surface snow cover we show that the effect of higher temperatures will clearly outweigh the effect of wintertime precipitation increases and that Alpine snow cover is projected to importantly decrease especially at low elevations. For the high-end RCP 8.5 scenario the latter will experience an almost complete loss of natural snow cover by the end of the century. These and a large number of further projected impacts of future Alpine climate change will challenge the adaptive capacity of the affected systems, and the present work provides a comprehensive and detailed assessment of the projected changes in their atmospheric forcing. It should however be noted that despite the large ensemble size employed here and despite the preceding model quality assessment, our results are subject to inherent limitations and uncertainties. Some of these concern the inability of 12.5 and 50 km resolution climate simulations to represent fine scale details of the complex Alpine topography. Others concern the rather conservative statistical post-processing approach employed here that, for instance, largely neglects model weighting and model bias adjustment. These issues will be covered by upcoming works employing, for instance, ensembles of convection-permitting climate simulations and possibly adding more detail to the broad but comprehensive picture provided in the present work.

**Supplementary Information** The online version contains supplementary material available at <https://doi.org/10.1007/s00382-022-06303-3>.

**Acknowledgements** The present work is based on the EURO-CORDEX regional climate model database. We thank all EURO-CORDEX modelling groups for making their simulations available. The main RCM ensemble employed in this work was assembled and thoroughly evaluated in the frame of the CH2018 Climate Scenarios for Switzerland. We thank the entire CH2018 crew for their contribution to this task, in particular Curdin Spirig for setting up and harmonizing the simulation database. We furthermore acknowledge the Swiss National Supercomputing Centre CSCS for providing storage and computing resources. The case study Ötztal Alps was funded by the Austrian Climate Research Program ACRP via the project “Future Snow Cover Evolution in Austria” (FuSE-AT, <https://fuse-at.ccca.ac.at/>).

**Funding** Funding was received from Klima- und Energiefonds (Austria).

**Data Availability** The EURO-CORDEX simulation data are available from the Earth System Grid Federation (ESGF; <https://esgf.llnl.gov>). The software code employed for the analysis is available from the authors upon request.

## Declarations

**Conflict of interest** The authors declare that they have no conflict of interest.

**Open Access** This article is licensed under a Creative Commons Attribution 4.0 International License, which permits use, sharing, adaptation, distribution and reproduction in any medium or format, as long as you give appropriate credit to the original author(s) and the source, provide a link to the Creative Commons licence, and indicate if changes were made. The images or other third party material in this article are included in the article's Creative Commons licence, unless indicated otherwise in a credit line to the material. If material is not included in the article's Creative Commons licence and your intended use is not permitted by statutory regulation or exceeds the permitted use, you will need to obtain permission directly from the copyright holder. To view a copy of this licence, visit <http://creativecommons.org/licenses/by/4.0/>.

## References

- Adler C, Wester P, Bhatt I, Huggel C, Insarov G, Morecroft M, Muccione V, Prakash A (in press) Cross-Chapter Paper 5: Mountains, in IPCC 6th Assessment Report, Working Group 2 “Impacts, adaptation and vulnerability” 2022 [https://report.ipcc.ch/ar6wg2/pdf/IPCC\\_AR6\\_WGII\\_CrossChapterPaper5.pdf](https://report.ipcc.ch/ar6wg2/pdf/IPCC_AR6_WGII_CrossChapterPaper5.pdf). Accessed 28 February 2022.
- Allen M, Ingram W (2002) Constraints on future changes in climate and the hydrologic cycle. *Nature* 419:228–232. <https://doi.org/10.1038/nature01092>
- Armstrong RL, Brun E (2008) Snow and climate: physical processes, surface energy exchange and modeling. Cambridge University Press, Cambridge
- Auer I, Böhm R, Jurkovic A et al (2007) HISTALP—historical instrumental climatological surface time series of the greater Alpine region. *Int J Climatol* 27:17–46. <https://doi.org/10.1002/joc.1377>
- Ban N, Schmidli J, Schär C (2015) Heavy precipitation in a changing climate: does short-term summer precipitation increase faster? *Geophys Res Lett* 42:1165–1172. <https://doi.org/10.1002/2014GL062588>
- Ban N, Rajczak J, Schmidli J, Schär C (2020) Analysis of Alpine precipitation extremes using generalized extreme value theory in convection-resolving climate simulations. *Clim Dyn* 55:61–75. <https://doi.org/10.1007/s00382-018-4339-4>
- Ban N, Caillaud C, Coppola E et al (2021) The first multi-model ensemble of regional climate simulations at kilometer-scale resolution, part I: evaluation of precipitation. *Clim Dyn* 57:275–302. <https://doi.org/10.1007/s00382-021-05708-w>
- Begert M, Frei C (2018) Long-term area-mean temperature series for Switzerland—combining homogenized station data and high resolution grid data. *Int J Climatol* 38:2792–2807. <https://doi.org/10.1002/joc.5460>
- Boé J, Somot S, Corre L, Nabat P (2020) Large discrepancies in summer climate change over Europe as projected by global and regional climate models: causes and consequences. *Clim Dyn* 54:2981–3002. <https://doi.org/10.1007/s00382-020-05153-1>
- Brogli R, Kröner N, Sørland SL, Lüthi D, Schär C (2019) The role of hadley circulation and lapse-rate changes for the future European





